Available online at www.sciencedirect.com
ScienceDirect
Geochimica et Cosmochimica Acta 74 (2010) 2212–2230
Geochimica et Cosmochimica Acta
www.elsevier.com/locate/gca

Metal in CR chondrites

John T. Wasson *,[1], Alan E. Rubin

Institute of Geophysics and Planetary Physics, University of California, Los Angeles, CA 90095-1567, USA

Received 22 October 2009; accepted in revised form 7 January 2010; available online 13 January 2010

Abstract

In section many low-FeO CR chondrules are surrounded by rings of metal; this metal-cladding seems to have formed during chondrule melting events as films of metal that wetted the surface. Electron microprobe studies show that in each ring the metal is very uniform in composition, consistent with efficient mixing during formation of the metal film. In contrast the mean Ni contents of 13 different rings vary by up to a factor of 2. There is no FeS associated with ring metal. Ring metal Co is positively correlated with Ni but the Co/Ni ratio seems to decrease with increasing Ni. We observed a weak negative correlation between ring metal Ni and the fayalite content of the host olivine. Coarse interior metal has higher Ni contents than that in the surrounding rings. At any specific chondrule location, smaller grains tend to have lower Ni contents than larger grains. These trends in Ni seem to reflect two processes: (1) The mean Ni content of metal (and easily reduced sulfides or oxides) in chondrule precursor materials seems to have decreased with the passage of time; on average, the metal in earlier-formed chondrules had higher Ni contents than the metal in later-formed chondrules. (2) Some oxidized Fe was reduced during chondrule formation leading to lower Ni contents in small grains compared to large grains; prior to reduction the Fe was in FeS or in FeO in accessible (fine-grained) sites. We suggest that the compositional evolution of nebular solids was responsible for the interchondrule variations whereas reduction of minor amounts of FeS or FeO was responsible for the size-related small variations in Ni content. We suggest that, during chondrule formation events, CR chondrules experienced relatively long thermal pulses that were responsible for the thorough loss of FeS and the common granoblastic texture observed in low-FeO chondrules. The preservation of the structures of internal rings shows, however, that even though high temperatures occurred in the secondary chondrule, temperatures in the centers of large (>20 μm) metal and silicate grains in the primary chondrule did not get high enough to cause appreciable melting.

1. INTRODUCTION

The CR chondrites are quite pristine. They have avoided parent-body thermal metamorphism; for example, metallic Fe–Ni has not recrystallized as mixes of kamacite and taenite. These meteorites have experienced minor asteroidal aqueous alteration, but the degree of alteration is less than that experienced by all CM chondrites. The aqueous alteration resulted in only minimal oxidation of coarse metal.

As recognized by Wood (1963), most of the metal in CR chondrites is associated with chondrules; especially challenging to understand is the type of chondrules that Wood designated as "armored", i.e., those with large amounts of coarse metal on their surfaces. Wood attributed the surficial metal to surface tension effects present during chondrule formation (by condensation in the solar nebula). Most recent researchers have attributed surficial metal distributions to centrifugal forces (e.g., Grossman and Wasson, 1985; Kong and Palme, 1999; Humayun et al., 2002).

Although Wood (1963) was impressed by the uniform compositions observed in the metal of CR Renazzo, more recent researchers have noted important differences and trends. Lee et al. (1992) noted that Ni and Co contents were generally higher for coarse interior grains than for those on chondrule surfaces. They also found that large grains

* Corresponding author. Tel.: +1 310 825 1986; fax: +1 310 206 3051.
E-mail address: jtwasson@ucla.edu (J.T. Wasson).
[1] Also Departments of Earth and Space Sciences and Chemistry and Biochemistry, University of California, Los Angeles, CA 90095, USA.

0016-7037/$ - see front matter © 2010 Elsevier Ltd. All rights reserved.
doi:10.1016/j.gca.2010.01.014

attached to chondrules were compositionally zoned, typically with lower Ni contents in their exteriors.

In their comprehensive paper on CR petrography, Weisberg et al. (1993) stated that the positive Ni vs. Co trend in CR chondrule metal follows the predicted compositional path for metal condensing from a gas of solar composition. Although condensation was their preferred model, they noted that it had problems explaining features such as the presence of volatile elements in chondrule interiors.

Kong et al. (1999) generated neutron-activation concentration data for magnetic separates of three CR chondrites; the magnetic fractions were separated into fine (<0.5 μm) and coarse fractions. They observed that concentrations of all siderophiles are higher in the fine fraction by factors that are typically about 1.1–1.6. Kong and Palme (1999) used neutron-activation analysis to study 18 silicate-rich chondrules, three metal-rich chondrites, two matrix samples and two rims in Renazzo. They observed relatively high Se in chondrules. Siderophile concentrations in the metallic chondrules were lower than in bulk Renazzo metal, consistent with the observed lower concentrations observed by Kong et al. (1999) in the coarse magnetic fraction.

Connolly et al. (2001) were the first to study a larger set of metal grains from the surfaces of individual chondrules. They used the SIMS (secondary ion mass spectrometry) technique developed by Hsu et al. (2000) to determine the PGE (platinum-group-elements) Os, Ir, Pt and Au in CR metal grains for which Fe, Ni, Co and Cr were determined by EMP (electron microprobe). They found highly variable contents of the PGE that they classified into two types, "normal" and "depleted". They attributed the latter to volatilization and recondensation, with the "depleted" grains having low contents of PGE.

Zanda et al. (2002) and Humayun et al. (2002) briefly described studies of CR metal in abstracts. Zanda et al. inferred that Fe was evaporated during chondrule melting; its recondensation on chondrule surfaces led to dilution of Ni and Co in the surficial metal. Humayun et al. reported ratios to Fe for Pd, Cu and Ni; Pd correlated with Ni, and Cu showed a wide range and a negative correlation with Ni.

2. SAMPLES AND PETROGRAPHIC TECHNIQUES

We studied polished thin sections of LaPaz Escarpment (LAP) 02342,12, Acfer 097 and Acfer 059. For convenience in this paper we will shorten these names to LAP, A97 and A59. Available evidence is consistent with the assumption that A97 and A59 are paired.

The UCLA LEO 1430 scanning electron microscope (SEM) was used to create back-scattered electron (BSE) images of the entire thin sections; these were combined into poster-size mosaics; a grid was superposed on the mosaic and used to label the chondrules and other features. Each square is subdivided into a 5 × 5 subgrid designated by letters. The top row has the letters **a** through **e**, with **a** at the upper left position.

A detailed BSE image was prepared for each studied chondrule. These are shown and discussed in Section 3.

Opaque phases were analyzed using the UCLA JEOL EMP. We determined four siderophiles (Fe, Co, Ni and Cr) with two or three other elements (S and Mg or Si) used to control the purity of phases. For metal and sulfide analyses, the standards were millerite for S, 99.99%-pure iron for Fe, and the Fe–Ni–Co alloy NBS 1156 for Ni and Co. Cobalt values were corrected for the interference of the Fe K_β X-ray peak with the Co K_α line; corrections for the Fe K_β interference are typically about as large as the reported values.

We analyzed all the large grains in chondrule interiors and between 15 and 48 points on each ring. Analyses were rejected if the totals were outside the range 97.5–101 wt.% or if the S or Mg content was >0.065 wt.%. Most rejected analyses were because of low totals. In LAP the fraction of rejected points was 3%. In A97 it was 8% and in A59 it was 20%. The latter sample was located near an exterior surface of the meteorite and had experienced moderate terrestrial oxidation.

Oxide phases were analyzed using the UCLA JEOL EMP. Natural and synthetic standards were used: chromite for Cr, forsterite for Si and Mg, albite for Na, Mn-rich garnet for Mn, orthoclase for K, millerite for S, grossular for Al and Ca, and magnetite for Fe. The beam current was limited to 15 nA to minimize loss of alkalis. We used ZAF corrections.

Means of numerous sets of metal data are listed in Tables 1–3. All data are reported in wt.%; to save space below we shorten this to % in the running text. The entire EMP data set is presented in Electronic Annex.

3. RESULTS AND DISCUSSION

3.1. Textural classification of CR metal

As shown in our complete image for LAP 02342,12 (Fig. 1 of Wasson and Rubin, 2009), a large fraction of CR metal is on the surfaces of chondrules. In the most photogenic cases, the metal forms a ring around the chondrule. To set the stage we show two "poster" chondrules in LAP.

LAP chondrule J5l (Fig. 1a) shows the simplest kind of metal-clad chondrule. This round 890 × 1060-μm-size type-I porphyritic olivine-pyroxene (POP) chondrule is surrounded by a broken ring of metal beads that are relatively uniform in thickness; the ring encompasses the entire periphery of the chondrule. The beads have long dimensions of 50–250 μm and thicknesses of ~50 μm. There are numerous metal masses in the chondrule interior: the smallest are ~2 μm in diameter; the four largest grains have long axes of 50–100 μm. Olivine phenocrysts (mean composition Fa2.7) are generally rounded and range in size from ~15 to 110 μm; some olivine grains occur as granoblastic clumps (up to 220 μm in size) with no intergranular mesostasis. Low-Ca pyroxene (mean composition Fs2.5Wo0.7) is generally restricted to the outer portion of the chondrule where it occurs as compacted grains with little mesostasis. There is a "smooth rim" around parts of the chondrule, consisting of relatively coarse (~10–20-μm-size) ferroan phyllosilicate grains and unaltered, underlying grains of silica and magnesian low-Ca pyroxene (Fs2.5–5.0 Wo0.7–1.2). What appears to be a fine-grained matrix-like rim merges with the chondrite matrix at several points and is unresolvable from

Table 1
Mean concentrations (bold) and standard deviations (in units of wt.%) for metal grains from 11 chondrule rings (or shells) from nine chondrules in three CR chondrites. The p rng and s rng column headings stand for primary and secondary rings, respectively. The number below the mean values is the number of points. The bottom line gives the composition of olivine in the host chondrule (in mol%).

Chondrite	LAP		LAP		LAP		LAP		LAP		LAP	
Cdrl, ring	F3o Mean	p rng Stdv	F3o Mean	s rng Stdv	J5l Mean	p rng Stdv	A6i Mean	p rng Stdv	F5s Mean	p rng Stdv	I5b Mean	p rng Stdv
Cr	**0.27**	0.09	**0.26**	0.08	**0.36**	0.06	**0.23**	0.06	**0.22**	0.07	**0.24**	0.05
Fe	**92.1**	0.4	**93.4**	0.3	**94.8**	0.5	**94.2**	0.5	**93.6**	0.6	**94.0**	0.4
Co	**0.32**	0.03	**0.25**	0.04	**0.22**	0.04	**0.23**	0.04	**0.22**	0.03	**0.26**	0.04
Ni	**7.16**	0.29	**5.39**	0.15	**4.48**	0.36	**4.76**	0.04	**5.38**	0.03	**5.23**	0.12
Total	**99.9**	0.4	**99.3**	0.3	**99.9**	0.3	**99.4**	0.4	**99.4**	0.7	**99.7**	0.4
n	20		15		23		21		26		17	
Oliv Fa	1.3		1.4		2.7		2.4		1.5		1.9	

Chondrite	A97		A97		A97		A97		A59		A59		A59	
Cdrl, ring	N5w Mean	p rng Stdv	N5w Mean	s rng Stdv	E3b Mean	p rng stdv	H11s Mean	p rng Stdv	E2n Mean	p rng Stdv	I4b Mean	p rng Stdv	I7m Mean	p rng Stdv
Cr	**0.28**	0.07	**0.28**	0.07	**0.25**	0.07	**0.39**	0.10	**0.30**	0.06	**0.22**	0.08	**0.48**	0.07
Fe	**92.9**	0.3	**93.5**	0.7	**93.5**	0.6	**93.2**	0.7	**93.5**	0.4	**92.4**	0.4	**91.4**	0.4
Co	**0.28**	0.03	**0.27**	0.04	**0.24**	0.04	**0.25**	0.03	**0.21**	0.03	**0.25**	0.03	**0.27**	0.03
Ni	**6.11**	0.16	**5.34**	0.24	**5.07**	0.38	**5.02**	0.39	**5.09**	0.13	**6.24**	0.26	**6.39**	0.21
Total	**99.6**	0.4	**99.4**	0.7	**99.1**	0.4	**98.9**	0.5	**99.1**	0.4	**99.1**	0.4	**98.5**	0.4
n	13		18		14		21		40		31		26	
Oliv Fa	1.7				1.6		1.2		2.5		2.2		1.0	

the matrix. As discussed by Wasson and Rubin (2009), this is the general case with fine-grained rims around LAP chondrules; they concluded that these features are actually interchondrule matrix and thus are not chondrule rims that were formed by accretion of individual grains in the nebula.

LAP chondrule F3o (Fig. 1b) is a 1850 × 1940-μm-size spheroidal chondrule with a long axis of ~1.8 mm. This is a concentric (i.e., nested) compound chondrule, a spheroidal chondrule inside a spheroidal chondrule shell. The primary type-I porphyritic olivine (PO) chondrule is surrounded by an interrupted ring of metal. Olivine phenocrysts in the primary chondrule (mean composition Fa1.3) are generally rounded and range in size from ~20 to 120 μm; as in J5 l, some olivine grains occur as clumps (up to 350 μm in size) forming a granoblastic texture with no intergranular mesostasis. The secondary chondrule shell is type-I POP with Fa1.4 olivine and Fs1.6Wo0.9 low-Ca pyroxene; it is surrounded by a ring of metal beads that has some big gaps in the SW. Surrounding the secondary shell is an igneous rim with a convoluted outline containing much fine-grained (ca. 10-μm diameter) metal and with only small arcs of what may be a thin exterior metal ring. There are numerous small (~2–5 μm) and several large (⩾40 μm) metal grains in the interior of the primary chondrule.

We classify CR metal into three main categories:

(1) *Metal associated with rings*. In the first category, we divide the metal from CR chondrules into primary rings (metallic shells around the first chondrule formed) and secondary rings (metallic shells around the secondary chondrule in concentrically compound chondrules). Although some chondrules show hints of tertiary rings we have not observed any that are sufficiently well defined to justify assigning a set of metal grains to such rings.

(2) *Coarse metal grains in chondrule interiors*. Interior grains range from submicrometer size to massive grains hundreds of micrometers across. The coarse grains (⩾40 μm) are adjacent to silicates and mesostasis, as opposed to being poikilitically enclosed within silicates.

(3) *Metal grains within igneous rims*. These grains are moderately uniform in size (e.g., ~3–40 μm in F3o), generally smaller than the largest grains in the rings or in chondrule interiors, and relatively uniformly distributed among the silicate grains. As first noted by Zanda et al. (2002), the igneous rims commonly have convoluted outer surfaces. Rubin and Wasson (2005) noted that many chondrules in CO chondrites also have convoluted (or lobate) outer surfaces.

Figs. 2 and 3 show images of the nine additional chondrules we studied that have rings of metal and one other chondrule (Fig. 2d) that has a very large metal grain attached to its side.

LAP chondrule A6i (Fig. 2a) is a 1610 × 1830-μm-size ellipsoidal type-I POP chondrule with olivine phenocrysts (mean Fa2.4) ranging in size from 20 to 160 μm; some of the phenocrysts occur in granoblastic clumps. Low-Ca pyroxene (mean composition Fs1.6Wo0.6) is restricted to the outer portions of the chondrule where it occurs in elongated grains up to 1 mm in length. Three large metal grains (80–310 μm) occur in the chondrule interior; two are partly surrounded by mesostasis but the smallest is completely enclosed (in two dimensions) by pyroxene. The chondrule is surrounded by a ring of metal lumps; the lumps range in thickness from 40 to 120 μm and in length from 40 to 550 μm. The ring encompasses the entire preserved periphery of the chondrule (an arc of ~90° is missing at the edge of the thin section).

Table 2
Means and standard deviations of large (⩾40 μm) interior metal grains in chondrules with metal rings. See footnote for abbreviations[a].

	LAP F3o Inner crse		LAP F3o Inner fine		LAP F3o Btw rings		LAP J5l Nod 1–3		LAP J5l Nod 5–8		LAP A61 Nod 2		LAP A61 Nod 1,3,4		A59 I4b Only nod		A97 E3b Nod 1		A97 N5w Nod 1	
	Mean	Stdv	Mean	Stdv	Mean	Stdv	Mean	Stdv	Mean	Stdv	Mean	Stdv	Mean	Stdv	Mean	Stdv	Mean	Stdv	Mean	Stdv
Cr	**0.23**	0.06	**0.21**	0.02	**0.22**	0.06	**0.27**	0.09	**0.20**	0.06	**0.17**	0.03	**0.27**	0.13	**0.17**	n.a	**0.12**	0.06	**0.211**	0.08
Fe	**91.8**	0.8	**91.2**	0.9	**92.0**	0.4	**91.9**	0.6	**92.3**	0.5	**86.2**	0.2	**92.2**	0.8	**89.0**	n.a	**81.1**	0.1	**87.5**	1.1
Co	**0.32**	0.04	**0.29**	0.03	**0.30**	0.04	**0.33**	0.04	**0.27**	0.05	**0.46**	0.03	**0.31**	0.02	**0.28**	n.a	**0.59**	0.04	**0.40**	0.09
Ni	**7.96**	0.21	**7.35**	0.21	**6.81**	0.55	**7.91**	0.37	**6.54**	0.24	**12.75**	0.11	**6.65**	0.28	**9.69**	n.a	**17.10**	0.10	**11.0**	1.69
Total	**100.3**	0.9	**99.1**	0.7	**99.4**	0.6	**100.5**	0.6	**99.5**	0.4	**99.8**	0.2	**99.7**	0.6	**99.1**	n.a	**98.9**	0.2	**99.2**	0.4
n	9		4		6		8		5		3		6		2		3		3	

[a] *Abbreviations:* crse, coarse; betw, between; nod, nodule(s); stdv, standard deviation.

Table 3
Means and standard deviations of large (⩾40 μm) metal grains in igneous rims and (the last three pairs of columns) chondrules with convoluted outer margins.

	LAP F3o		LAP K3l		LAP I1w		LAP H7c		A59 E2n		A59 I4b		A59 I7m		LAP C4q		LAP G2a		LAP H7c	
	Mean	Stdv	Mean	Stdv	Mean	Stdv	Mean	Stdv	Mean	Stdv	Mean	Stdv	Mean	Stdv	Mean	Stdv	Mean	Stdv	Mean	Stdv
Cr			**0.17**	0.12					**0.25**	0.07	**0.19**	0.07	**0.51**	0.07	**0.24**	0.05	**0.37**	0.04	**0.39**	0.03
Fe	**92.9**	n.a.	**94.6**	0.6	**94.4**	n.a.	**94.8**	0.27	**93.8**	0.24	**92.5**	1.0	**91.3**	0.45	**95.2**	0.51	**92.7**	0.91	**93.7**	1.0
Co	**0.26**	n.a.	**0.28**	0.06	**0.28**	n.a.	**0.26**	0.02	**0.19**	0.03	**0.24**	0.04	**0.27**	0.02	**0.28**	0.04	**0.33**	0.04	**0.27**	0.03
Ni	**6.44**	n.a.	**5.55**	0.66	**5.93**	n.a.	**5.45**	0.07	**4.79**	0.28	**6.01**	0.70	**6.56**	0.15	**5.65**	0.63	**6.90**	0.66	**5.35**	0.17
Total	**99.6**	n.a.	**100.9**	0.2	**100.5**	n.a.	**100.5**	0.3	**99.1**	0.6	**98.9**	0.5	**98.6**	0.5	**101.6**	0.4	**100.6**	0.7	**100.1**	0.9
n	2		2		2		5		11		17		12		6		7		4	

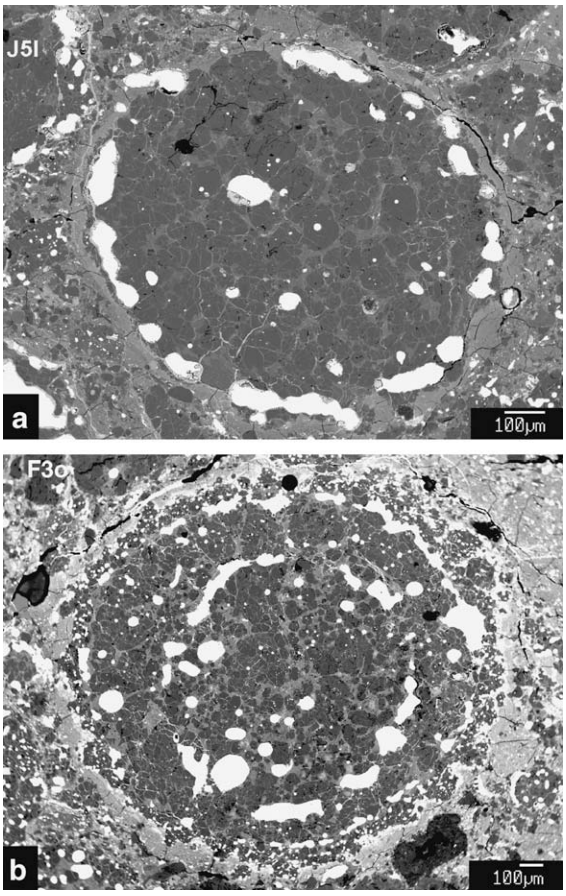

Fig. 1. Back-scattered-electron (BSE) images of two chondrules with metal rings in CR LAP 02342. (a) Chondrule J5l shows a near-circular shape and a largely symmetric ring of metal beads. (b) Chondrule F3o is a concentric compound chondrule with a symmetric inner ring and an outer ring of variable bead thickness.

LAP chondrule F5s (Fig. 2b) is a 1340 × 1410-μm-size spheroidal type-I POP chondrule with coarse phenocrysts and phenocryst clumps (olivine Fa1.5, low-Ca pyroxene Fs2.6Wo0.5) up to 600 μm in maximum size. Mesostasis occurs as elongated patches adjacent to elongated mafic silicate phenocrysts in the chondrule interior. Only minor amounts of metal occur in the chondrule interior (as rounded blebs 5–25 μm in diameter). The chondrule is surrounded by a broken ring of coarse metal lumps (ranging in thickness from 50 to 150 μm and in length from 30 to 450 μm).

LAP chondrule I5b (Fig. 2c) is an ellipsoidal barred olivine (BO) chondrule 1080 × 1230 μm in size with continuous and broken olivine bars 20–45-μm thick that have an average composition of Fa1.9. It is adjacent to a fragment of another BO chondrule (H5o). In I5b, minor amounts of moderately calcic low-Ca pyroxene (Fs1.5Wo2.4) occur between some of the olivine bars; a large (~100 μm) pyroxene mass (Fs1.4Wo3.4) occurs near the WSW part of the chondrule. Metal is absent from the I5b interior and occurs only in a broken ring within and at the outer surface of a 100–125-μm-thick olivine shell that surrounds the interior. The metal grains in the ring range in thickness from 15 to 100 μm and occur as isolated beads and as elongated clumps up to 500 μm long.

We originally thought that the adjacent BO chondrule (now called H5o, 480 × 720 μm) was a displaced fragment of chondrule I5b. However, when we measured phase compositions in H5o we found that it differed in metal and silicate compositions. The olivines are appreciably lower in FeO (Fa1.0 ± 0.3 in H5o) and nine of the smallish metal beads in the incomplete ring have the lowest Ni values we encountered, mean 3.56%, standard deviation 0.34% Ni. In contrast, the Ni in the I5b ring has 5.23% Ni. The olivine bars are more regular in H5o and there is much less metal at the chondrule surface than in I5b. In addition, H5o does not contain pyroxene. It seems clear that the two BO chondrules had independent origins.

A97 chondrule N4n (Fig. 2d) is a 910 × 1610-μm-size type-I porphyritic pyroxene (PP) chondrule with 250–350-μm-size pyroxene phenocrysts (Fs3.1Wo0.3) and only minor amounts of mesostasis. The chondrule consists of a 750-μm-thick silicate hemisphere forming a moderately sinuous boundary with a very coarse metal grain 570 × 1000 μm in size. This single metal grain constitutes nearly half of the chondrule area in the plane of the thin section. A few small metal grains (6–25 μm) occur in the chondrule interior and another fairly coarse metal grain (110 × 250 μm) occurs on the opposite side of the chondrule at the surface.

The large metal grains shown in Fig. 2e, f and g are discussed in Section 3.4.

A97 chondrule N5w (Fig. 3a) is a 1760 × 1820-μm-size ellipsoidal type-I POP chondrule with mean olivine and low-Ca pyroxene compositions of Fa1.7 and Fs1.6Wo0.9, respectively. Rounded, quasi-equant and elongated phenocrysts are present, ranging in maximum dimension from 110 to 1200 μm. A single large (310 μm) moderately rounded metal grain occurs in the chondrule interior. The chondrule is surrounded by a broken inner ring of metal lumps that encompasses ~270° of arc. The lumps are ~80 μm thick and 110–370 μm long. The secondary POP shell is ~100 μm thick and is itself surrounded by a broken non-continuous ring of metal blebs that are ~40 μm thick and 20–180 μm long.

A97 chondrule E3b (Fig. 3b), located at the edge of the section, is a 940 × 1070-μm-size ellipsoidal type-I PO chondrule with 40–210-μm-size olivine phenocrysts with a mean composition of Fa1.6. The mesostasis is restricted to the chondrule center; the outer portion of the chondrule consists of massive olivine grains. The interior of the chondrule contains one moderately large (160 μm) rounded metal grain partially surrounded by mesostasis and a few tiny (1–8 μm) grains, most of which occur as inclusions within olivine. The chondrule is surrounded by a broken ring having only a few coarse metal lumps, ranging in thickness from 20 to 90 μm and in length from 15 to 120 μm.

A97 chondrule H11s (Fig. 3c), also located at the edge of the section, is a 2130 × 2370-μm-size ellipsoidal type-I PO chondrule containing 80–430-μm-size olivine phenocrysts with a mean composition of Fa1.3. Mesostasis occurs throughout the chondrule. The chondrule is surrounded by a near-continuous ring of coarse metal lumps; the lumps range in thickness from 20 to 190 μm and in length from 40 to 690 μm.

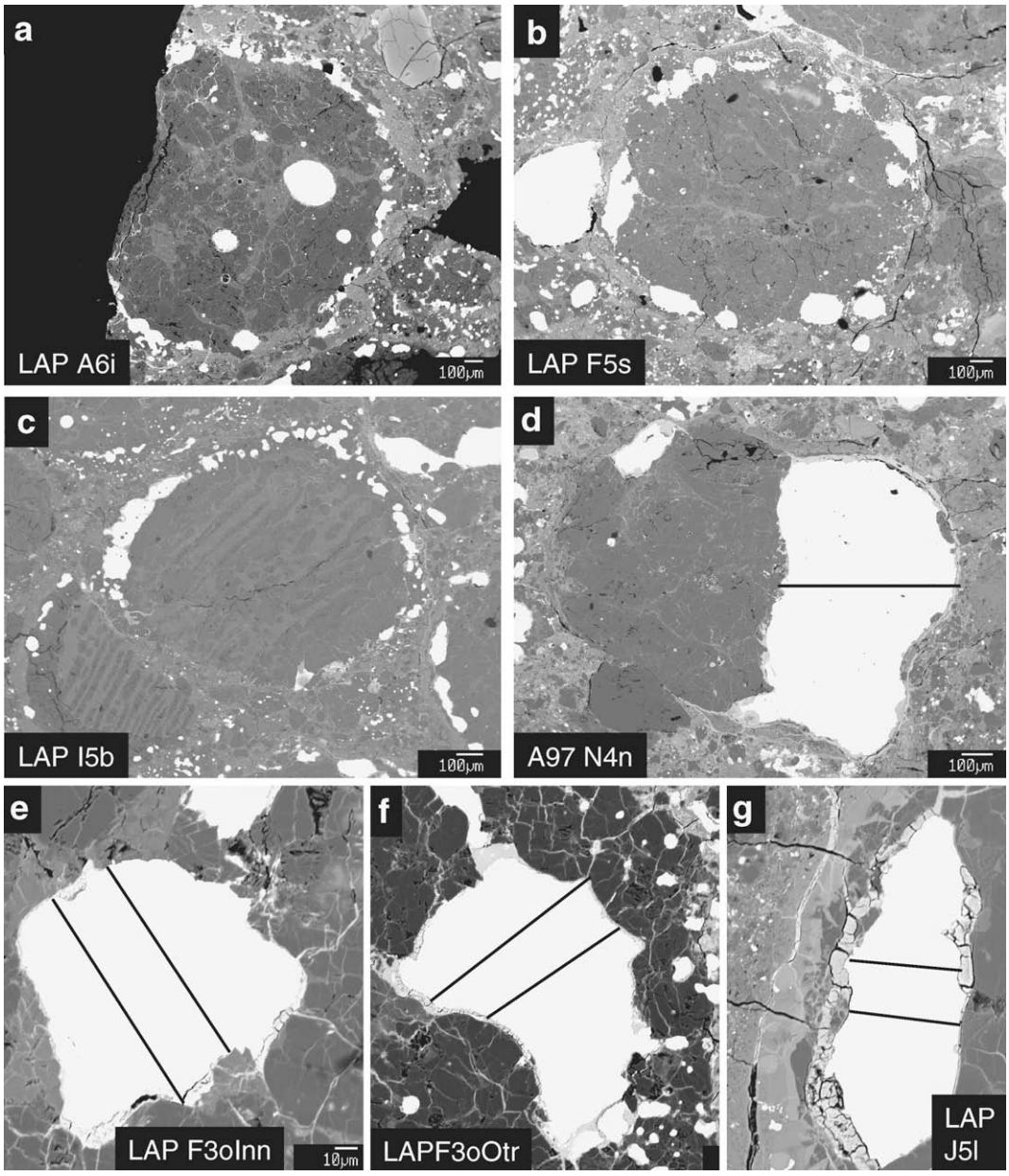

Fig. 2. BSE images of three LAP chondrules with metal rings and of four large metal nodules on which compositional profiles were carried out. (a) The ring around chondrule A61 is complete for the extant portion of this chondrule at the edge of the section; the 130 μm nodule just below the chondrule center contains 12.8% Ni, the other three large grains all contain about 6.6% Ni, and the ring metal contains 4.8% Ni. (b) The ring around chondrule F5s contains relatively few but large metal beads, (c) the ring around chondrule I5b is asymmetric, with >90% of the metal on the upper half; it has very uniform Ni (5.2%, 2% relative standard deviation. (d) Very large metal nodule on the right side of A97 chondrule N4n; the Ni content of the outer part of the profile is ~15% lower than that of the interior portion. (e) Parallel profiles were made on a grain at the SE part of the primary ring of LAP chondrule F3o. (f) Locations of parallel profiles on a large grain on the ENE of the secondary ring of chondrule F3o; the profile on the right is about 115 μm long. (g) The lines show the locations of profile tracks in a large metal bead on the left side of LAP chondrule J5l; a smooth rim is visible on the left side of the metal bead; the lower profile is about 55 μm long.

A59 chondrule E2n (Fig. 3d) is a 1330 × 1390-μm-size quasi-equant type-I POP chondrule with average olivine and low-Ca pyroxene compositions of Fa2.5 and Fs3.0Ws0.7, respectively. Phenocrysts range in size from 110 to 270 μm. Mesostasis occurs in large patches, mainly confined to the chondrule center. The chondrule is surrounded by a nearly continuous ring of coarse metal lumps (20–130 μm thick and 15–470 μm long). An igneous rim of varying thickness (80–360 μm) that contains abundant metal grains, 2–80 μm in size, surrounds the chondrule.

A59 chondrule I4b (Fig. 3e) is a 1200 × 1250-μm-size ellipsoidal type-I PO chondrule with rounded and clumped

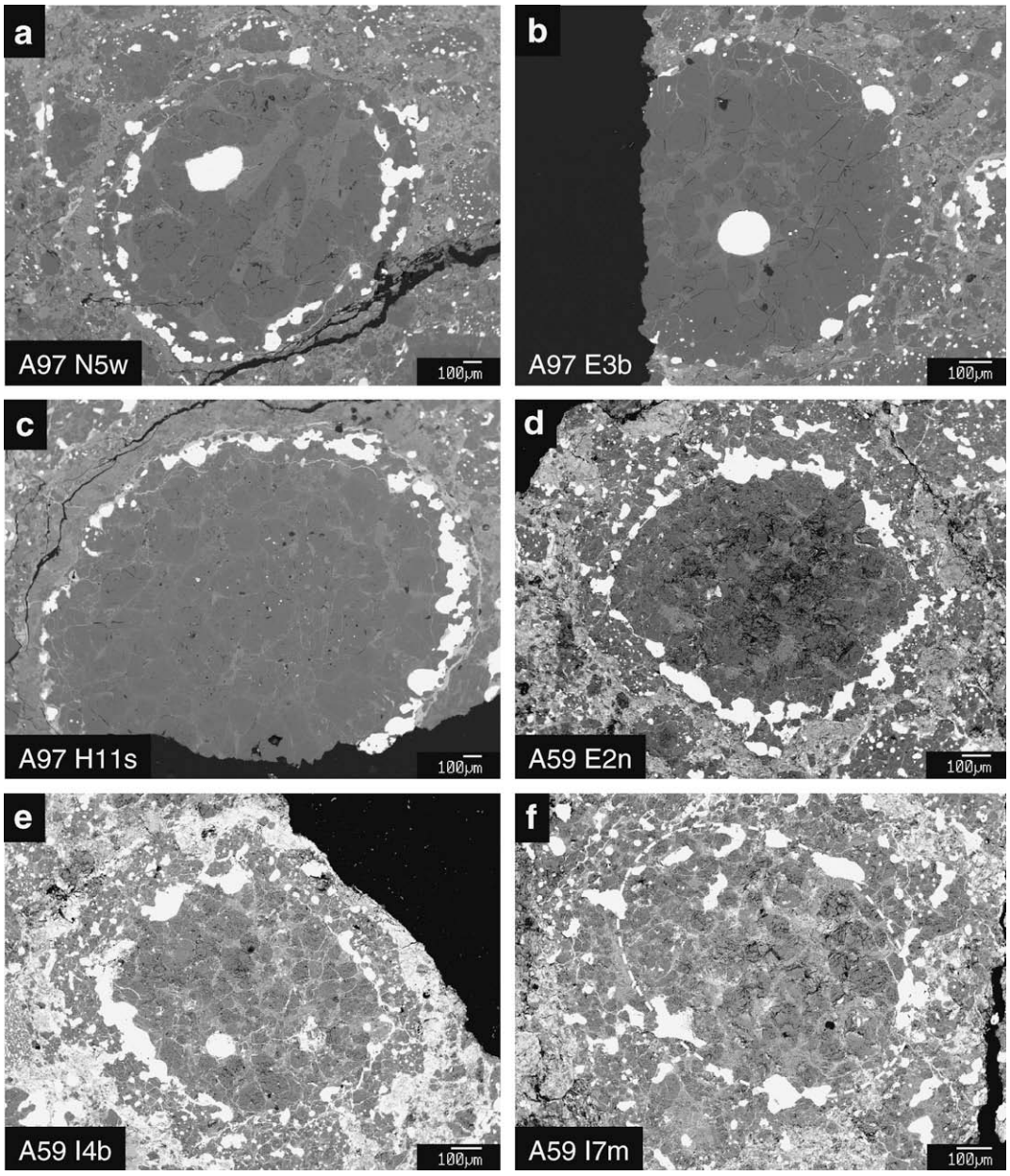

Fig. 3. BSE images of six chondrules with metal rings (three from A97 and three from A59). (a) A97 chondrule N5w has two rings; although these are close together, the Ni contents are well resolved; (b) the ring of A97 chondrule E3b consists of many grains about 40 μm in size and a few grains that are much larger; (c) part of A97 chondrule H11s is missing at the edge of the section; its ring is strongly asymmetric with the metal grains in the NE part being several times larger than those in the SW part. (d) A59 chondrule E2n has a roughly symmetric ring and is surrounded by a large igneous rim. (e) A59 chondrule I4b has an asymmetric primary rim, with most of the metal on the west side; it is surrounded by an igneous rim that is enriched in fine metal in its outer portions. (f) A59 chondrule I7 m has what appears to be a roughly ellipsoidal ring; the dashed curve shows the approximate location. The Ni contents are uniform for the coarse metal whether on the ellipse or inside it.

40–150-μm-size olivine phenocrysts with an average composition of Fa2.2. Mesostasis is moderately abundant and is present throughout the chondrule. One coarse (~90 μm) rounded metal grain and rare small (~3 μm) metal grains occur in the chondrule interior. A broken ring of coarse metal lumps (with a sparsely populated region in the SE) occurs around the chondrule; the lumps range in thickness from 20 to 130 μm and in length from 20 to 370 μm. The chondrule is surrounded by an igneous rim that varies from 90 to 210 μm in thickness; numerous 3–70-μm-size metal grains occur throughout the rim.

A59 chondrule I7 m (Fig. 3f) is an ellipsoidal 1330 × 1370-μm-size type-I PO chondrule with 30–130-μm-size olivine phenocrysts with a mean composition of Fa1.0. Mesostasis occurs throughout the chondrule. One 40 × 110-μm-size metal grain occurs in the chondrule interior; the remaining

metal occurs as an irregular discontinuous ring around the chondrule periphery. A dashed ring defines the location of the metal grains we interpret to be parts of a primary ring. The coarse metal lumps in the ring range in thickness from 20 to 130 μm and in length from 30 to 200 μm. The chondrule is surrounded by a 100- to 300-μm-thick igneous rim that contains 15- to 60-μm-size metal grains.

3.2. Composition of coarse metal rings on CR chondrules

In Table 1 we list mean concentrations and standard deviations for nine primary rings and two secondary rings. The standard deviations for Ni are quite small. Relative standard deviations (i.e., the standard deviation divided by the mean concentration) for Ni range from 2.6% in the primary ring for A97 chondrule N5w to 8.0% in the primary ring for LAP chondrule J5l.

The relative standard deviations for the minor elements Co and Cr are larger than those for Ni. Those for Co range from 8.5% to 16.1%, and those for Cr range from 15% to 38%. Although these latter values may seem high, it must be recognized that the Co concentrations are very low, that random errors are introduced by the correction for interference by the Fe K_β line, and that Cr is not siderophile at low temperatures. The degree of scatter in Cr values is low for EMP analyses of chondrule metal.

It is commonly stated that CR chondrites have avoided thermal metamorphism. The facts that appreciable Cr remains in the metal and has not partitioned into more stable phases such as chromite supports this interpretation.

Although the Ni data for each ring show relatively little scatter, the mean Ni contents show a large range from a low of 4.5% (and as low as 3.6% in nine relatively small beads for BO fragment H5o discussed above) in the primary ring of LAP chondrule J5l to a high of 7.2% in the primary ring of LAP chondrule F3o. These Ni differences are illustrated in Fig. 4; the errors attached to the points are mean 95% confidence limits based on the Student's *t* approach. The actual confidence limits for each ring point range from about 2/3 to 3/2 of these plotted values. The small confidence limits suggest that homogenization of the metal in each ring has occurred. The ring-to-ring differences in mean Ni show that the process responsible for homogenization of the metal shells for each chondrule did not cause homogenization among all the chondrules of the CR set. A parent-body process such as elemental diffusion facilitated by thermal metamorphism cannot be responsible.

Earlier studies (Lee et al., 1992; Weisberg et al., 1993) demonstrated that interior metal grains in CR chondrules have higher Ni contents than the metal on the surface. This observation is supported by the fact that, in the two chondrules that had both primary and secondary rings (LAP F3o and A97 N5w), the Ni content of the interior (primary) ring is resolvably higher than that of the secondary ring (Table 1, Fig. 4). There is little doubt that secondary rings were formed in a second melting event that resulted in the addition of largely molten silicates and metal that left the original, primary chondrule and its metallic shell relatively unaltered. This suggests the possibility that, with the passage of time, the Ni content of the metal in chondrule precursor materials was decreasing.

Past studies (e.g., Weisberg et al., 1993) have shown that Co and Ni are positively correlated in CR metal. In Fig. 5a we show that our ring data also show a positive correlation. The straight line is only for reference; it shows the locus of a possible line representing a constant Co/Ni ratio. Although the typical standard deviations (e.g., of 0.03–0.04 in Co) are large enough to permit a constant ratio, a line with a lower slope and a positive intercept is statistically more probable.

There are resolvable differences in the Cr contents of the rings. The maximum Cr concentration is 0.48% in the primary ring of A59 chondrule I7m, the minima are 0.22%

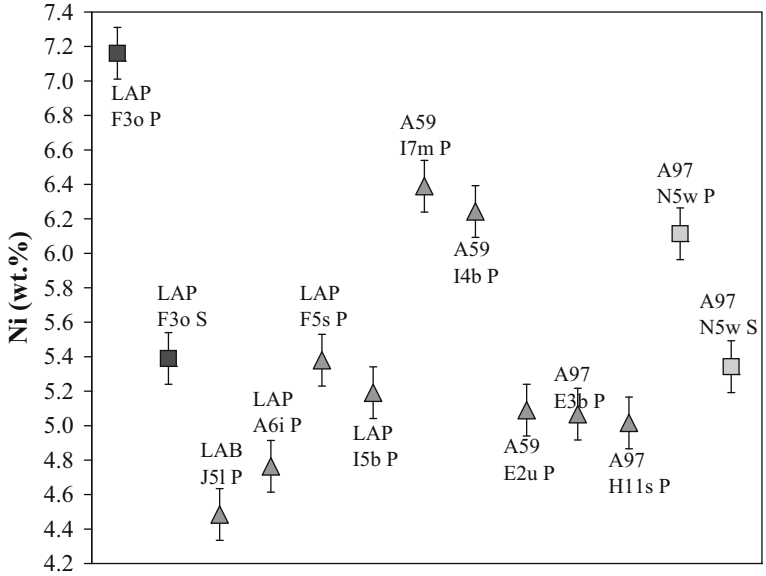

Fig. 4. The Ni contents of metal in 13 rings range from 4.4 to 7.2 wt.%. Two chondrules with inner and outer rings are shown with different symbols. The error bars show mean 95% confidence limits for the rings. Limits for individual rings range from 2/3 to 3/2 of these values. The two sets of square symbols show the Ni contents of primary rings (on the left) and secondary ring (on the right) for two compound chondrules.

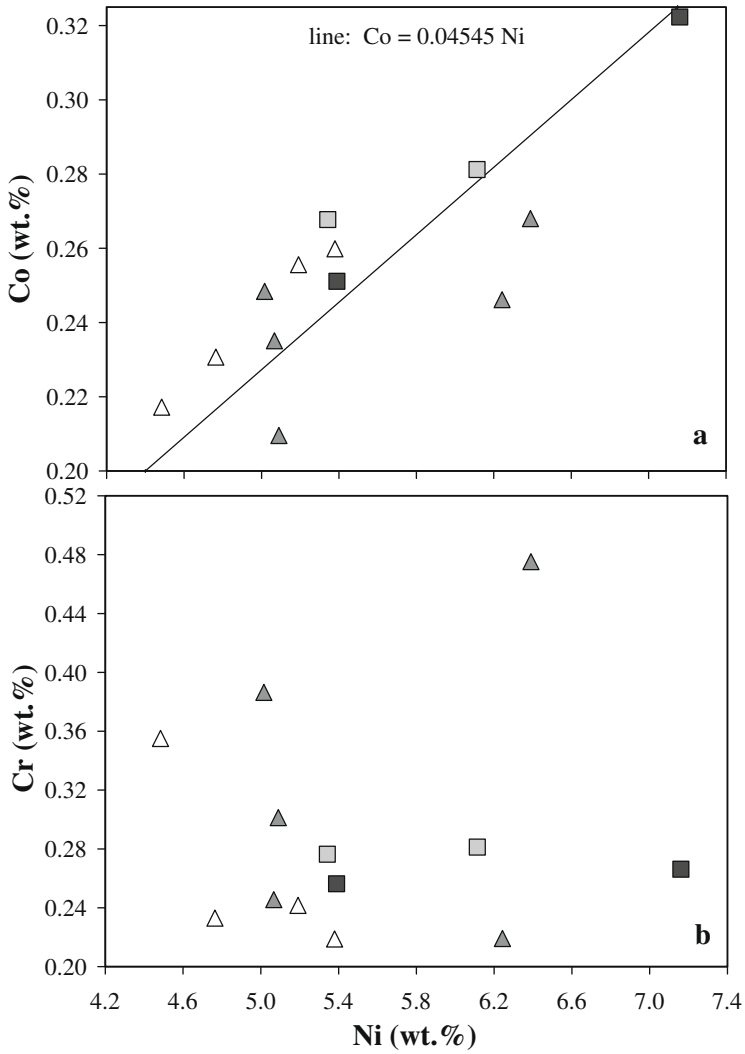

Fig. 5. (a) Contents of Co and Ni are positively correlated. The reference line shows a constant Co–Ni ratio; the trend of the data clearly yields a lower slope, but Co errors are large. (b) Contents of Cr and Ni are not correlated.

and 0.23% in the primary rings of chondrule A59 I4b and A97 E3b, respectively. The 95% confidence limits on these values are about 0.04 wt.%. In Fig. 5b we plot Cr vs. Ni for the rings. There is no evidence of a relationship between these two elements. Although, as Weisberg et al. (1993) noted, the Cr contents of CR metal are higher than those in most chondrites, the Cr/Fe ratios in the metal are nonetheless about 4–5× lower than mean ratios in whole-rock CR chondrites (Kallemeyn et al., 1994). Thus, the bulk of CR Cr is in phases other than metal. Because Cr is easily oxidized, one possible reason that it varies independently of Ni is that the fraction present as oxides varies as a function of redox conditions in the precursor materials. It is interesting that there is no resolvable variation in the Cr contents of the two sets of primary and secondary rings (in LAP F3o and A97 N5w), consistent with similar redox conditions when the individual chondrule melting events occurred.

As discussed, various authors have proposed that the Co–Ni correlation in CR metal is the result of FeO reduction and dilution by metallic Fe. It is therefore relevant to examine the relationship between the Ni in the metallic rings and the fayalite content of olivine in the host chondrule. Such a comparison (Fig. 6) shows that there is a significant negative correlation between olivine Fa and metallic Ni, the opposite of that expected from a model in which the variable Co and Ni are produced by variable degrees of reduction from similar precursor materials. This shows that such a model is not tenable. Most other reduction models, e.g., one involving reduction of FeO in interchondrule matrix, would predict no correlation between olivine Fa and metallic Ni. Models involving the evolution of nebular components are generally consistent with the negative trend. A closer look at such a scenario is presented in Section 4.

3.3. Compositions of coarse chondrule interior metal (inside the rings)

If there was coarse ($\geqslant$40 μm) metal inside the studied chondrules we included it in our studies. In most cases there were, at most, a few grains, but in some cases more grains

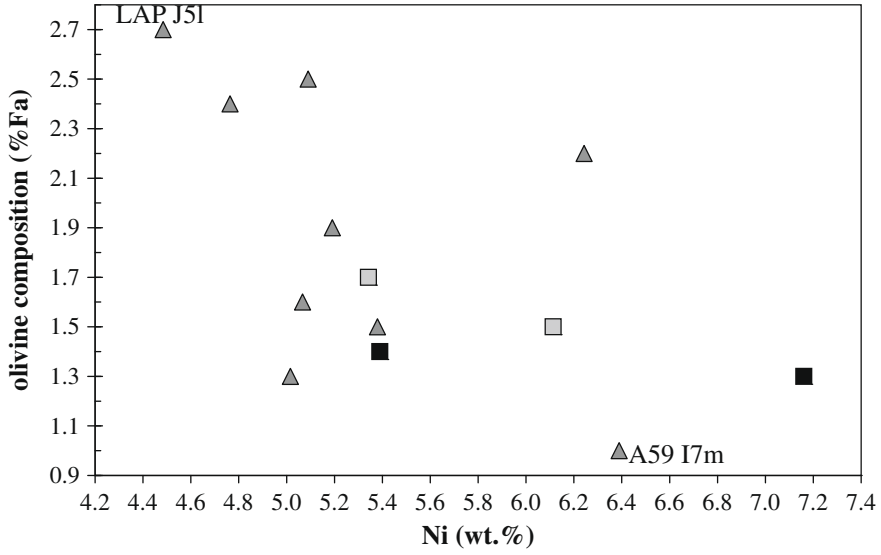

Fig. 6. A negative trend but much scatter is observed between the olivine Fa content of the host chondrule and the Ni content of the surrounding metal ring. This trend is the opposite of that expected from a scenario in which the range in metallic Ni contents is the result of the reduction of starting materials having high-Ni in the metal and high FeO in the silicates.

were present. Mean data for several sets of grains are summarized in Table 2.

There were many coarse interior grains in LAP chondrule F3o (Fig. 1b); in Table 2 we divided these into three categories: (a) coarser grains inside the primary ring; (b) finer grains inside the primary ring; and (c) grains located between the primary and secondary rings. In Table 3 we list a mean value for the metal grains scattered through the igneous rim outside the secondary ring.

The coarser (60–120 μm) interior metal in LAP F3o has a mean Ni content of 7.96%, much higher than the value of 7.16% measured in the primary ring. The finer (20–30 μm) interior metal has an intermediate mean Ni content of 7.35%, marginally higher than the mean of the primary ring and with several points overlapping in composition. Five of the six grains in the region between the two rings have compositions similar to that in the primary ring; the sixth has a Ni content of 5.9%, intermediate between the mean compositions of the rings and not overlapping with the data obtained for either set. Thus, in chondrule F3o we observe a monotonic sequence of Ni decreasing from (a) coarser interior metal to (b) finer interior metal to (c) primary ring metal to (d) metal between the rings to (e) secondary ring metal. As discussed below, the Ni contents of metal in the F3o igneous rim do not follow the trend; the mean Ni content of the rim is higher than that in the secondary ring.

There were also several coarse interior grains in LAP J5l. We divided these into two categories: The first cluster includes the two largest grains (90 and 60 μm) and a nearby 40 μm grain, all relatively near the center of the chondrule. The second set consists of four grains, 30–40 μm in size, scattered around the chondrule and relatively close to the primary ring. The larger and deeper (more centrally located) grains have higher Ni, Cr and Co than the more exterior and smaller grains. Although the compositions of the latter are higher in Fe than the former, the Ni contents of these finer and more exterior grains (6.5%) are still much higher than those of the primary ring. J5l thus also shows a monotonic trend of Ni decreasing from large grains near the center to intermediate grains near the periphery to the external metallic shell.

3.4. Profiles across coarse metal grains

Lee et al. (1992) measured Ni and Co profiles across several very large metal grains associated with chondrules. They reported that the profiles in chondrule interior grains are flat, but they observed small (10–15%) decreases in Ni concentrations (and smaller and less-well resolved decreases in Co) in the outer (matrix) side of large metal grains attached to chondrules.

We measured profiles across four coarse metal grains. The three smaller grains were members of chondrule rings, with one each from the inner and outer ring of LAP F3o and one across the largest ring grain in the primary ring of LAP J5l; the profile tracks are shown in Fig. 2e, f and g. We measured parallel profiles for each of these tracks and observed minor scatter but no resolvable change in Ni contents from inside to outside (Fig. 7).

We carried out a single profile across the very large (600-μm) metal grain that forms the right half of chondrule N4n in A97 (Fig. 2d). The profile is shown in Fig. 8. The Ni content is essentially constant (at about 5.7% Ni) for 75% of the profile on the side adjacent to the chondrule silicates but falls to a value of 4.9% Ni at the external surface. The interior/exterior Ni ratio is 1.16. The best explanation of this profile appears to be fractional crystallization. The diagram also shows a Co profile across the grain, but the uncertainty in the individual values is too high to allow a trend to be resolved. We assume that the Ni gradients observed in very large grains by Lee et al. (1992) also reflect fractional crystallization.

As discussed below, the Ni solid/liquid partition ratio is ~0.8 to 0.9 in S-free metallic melts of the sort present on the

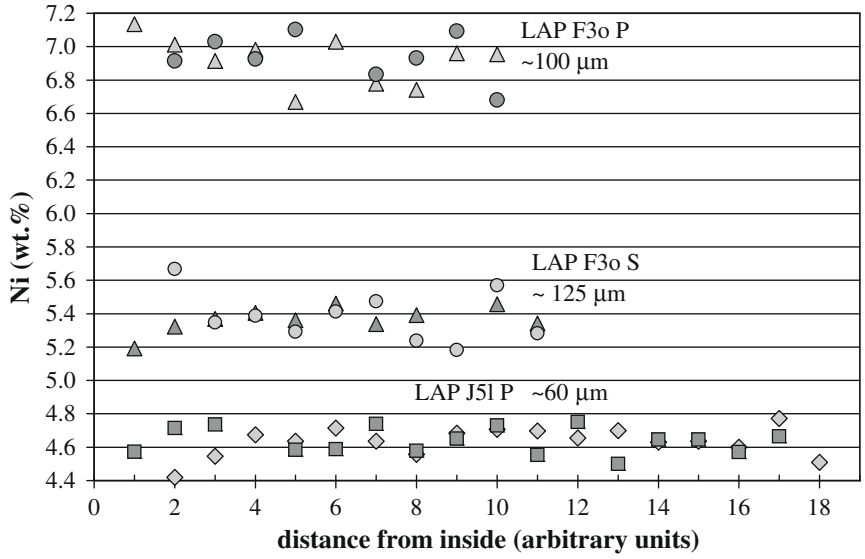

Fig. 7. Parallel profiles across three large grains from the primary and secondary rings in chondrule F3o and from the primary ring in J5l. The positions of the profiles are shown in Fig. 2. The profiles start at the interface between the host chondrule and the metal grain and extend radially outwards. There is no resolvable change in the Ni content along the tracks of these profiles. Point spacing varied among the profiles. Missing points were rejected because of low totals.

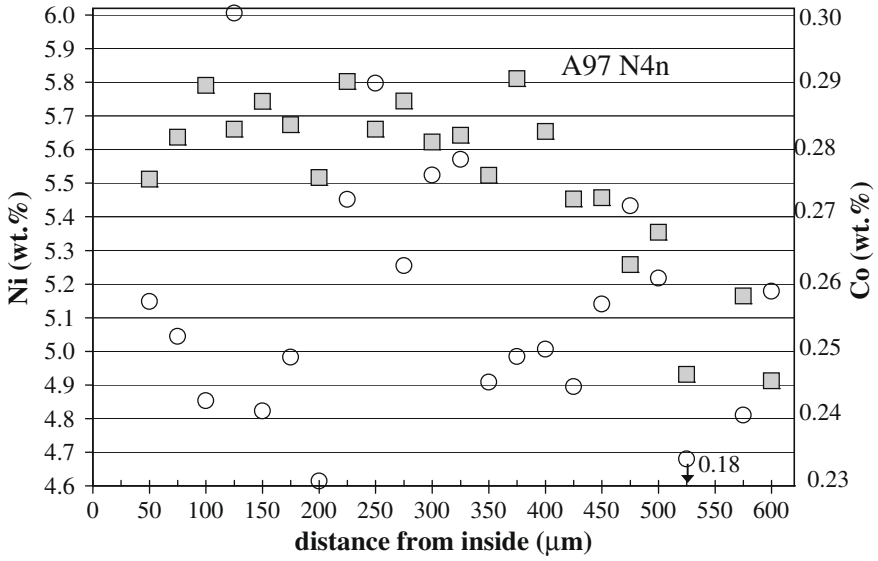

Fig. 8. A Ni profile across a very large metal grain on the right side of A97 chondrule N4n shows a resolvably lower Ni content on the outside. This appears to be the result of fractional crystallization. The location of the profile is shown in Fig. 2d.

surfaces of low-FeO CR chondrules (e.g., Chabot and Jones, 2003). Although ideal fractional crystallization would not occur in a rapidly cooling metal droplet, we will later present arguments indicating that the CR chondrules cooled more slowly than chondrules in other groups, and that moderate mixing of the residual liquid was possible.

3.5. Metal in igneous rims and simple chondrules with convoluted outer margins

A large fraction of CR chondrules is surrounded by an igneous rim with a convoluted outer margin; such an igneous rim surrounds the compound chondrule LAP F3o (Fig. 1b). There is also a large fraction of simple CR chondrules with textures very similar to those of igneous rims with dispersed metal and convoluted outer margins; these were first mentioned in Zanda et al. (2002).

The metal in these chondrules and rims typically has squiggly shapes, similar to objects common in paintings by Joan Miró. Texturally similar chondrules in CO chondrites were described by Rubin and Wasson (2005). The CR igneous rims and the chondrules with convoluted outer margins seem to have formed in the same way, by low degrees of melting during chondrule flash-heating events. For simplicity we will combine these into the category "convoluted-margin chondrules" or convoluted chondrules for short.

Concentrations in coarse metal in these convoluted chondrules are listed in Table 3. The total range in Ni is 4.8–6.6% in the igneous rims, going up to 6.9% in the convoluted chondrule LAP G2a; this is similar to the range observed in the rings. In most of the metal-clad chondrules there is a decrease in Ni from the interior grains to the exterior rings. As discussed above, in the double-ringed chondrule LAP F3o the Ni contents drop monotonically from interior to the primary ring to between the rings to the secondary ring. However, in the F3o igneous rim the Ni content is 6.4%, much higher than the concentration of 5.4% in the secondary ring. Although statistics are still limited, it appears that the compositions of igneous rims, the last material to be added to the chondrules, varied independently of the host chondrule.

It appears that there is more scatter (on average, higher standard deviations) in the metal in the convoluted chondrules and igneous rims compared to ring metal. Thus, although the compositions are rather uniform, the ring metal has been mixed more efficiently. Our convoluted chondrule and igneous rim data set is relatively small, so this conclusion is tentative.

3.6. Relation between metal composition and grain size

We find convincing evidence that, within a set of closely related metal grains, the smaller grains have lower Ni concentrations. For example, in the primary ring around chondrule A97 E3b we obtained good data for 14 points on 12 grains. The mean Ni concentration in the three smallest grains (25–30 μm in diameter) was 4.36%. The mean Ni content of the 11 largest grains (40–90 μm) was 5.07% (these are the data tabulated in Table 1). There is no doubt that all these grains are members of the rings. The small and large grains are both interspersed around the periphery; thus, geography plays no role in this trend.

In the primary chondrule of LAP F3o the Ni contents of nine points on coarser (50–80 μm) interior metal grains is 7.96%, significantly higher than the value of 7.35% found for four points on finer (25–40 μm) interior metal grains (Table 2). In the classic ringed chondrule LAP J5l the mean Ni content for eight points measured on grains of coarser interior metal is 7.91%, whereas that found in five grains of finer interior metal was 7.54% (Table 2). The largest grain (90 μm) and the smallest grain (25 μm) for which we have data are near one another in the center of the chondrule, about 300 μm from the beads of the overlying ring; the large grain (nodule 1) has 8.2% Ni; the small grain (nodule 8) has 6.4% Ni.

We were not able to resolve a relationship between size and composition in the metal grains embedded in igneous rims. As discussed in the previous section, there is moderate scatter among these grains. Thus we do not know whether this indicates that metallic Fe was added to grains in the igneous rims or whether the higher degree of scatter has obscured a possible size-compositional relationship. Our conclusion is that metallic Fe (probably mainly as a result of reduction of FeS) has been added to the metallic shells of chondrules and to the grains interior to these shells. It may or may not have been added to metallic grains in igneous rims.

3.7. A reduced chondrule with Si dissolved in the metal

LAP chondrule H2q has abundant Si in kamacite; Si contents range from 2.65% to 2.90%. The metal grains are round, relatively uniform in size (10–50 μm) and more or less uniformly dispersed. No other investigated CR chondrule has this texture or appreciable Si in their metal (i.e., their Si concentrations are all <0.1%). The reduced nature of chondrule H2q is also evident in its silicate compositions: Fa0.27 and Fs0.94Wo0.71; these values are more magnesian than those in the other CR chondrules. Although a few metal grains occur at the surface of chondrule H2q, there is no metal ring.

4. MODELS TO ACCOUNT FOR THE PROPERTIES OF CR METAL

In Table 4 we list 16 features of CR metal that require explanation. Because we (and earlier researchers) see no evi-

Table 4
Features of CR metal that require explanation.

1	A large fraction of CR metal resides on the surfaces of low-FeO chondrules
2	Much of the surface metal is roughly isotropically distributed
3	The surficial metal is now present typically as coarse ($\geqslant$50 μm) globules
4	In the vast majority of cases, there is essentially no FeS associated with surficial metal, and no FeS in the interiors of the host chondrules
5	On each chondrule surface, metal is uniform in composition
6	Surface metal composition varies from chondrule to chondrule and from shell to shell within concentric compound chondrules
7	Mean compositions of surficial shell metal show a positive Co-Ni correlation
8	There is no correlation between Cr and Ni in the mean compositions of surficial shell metal
9	Although Cr contents are high in CR metal, only ~10% of CR Cr is sited in metal
10	Ni concentrations of surface metal are negatively correlated with the fayalite contents of host chondrule olivine
11	Large interior metal grains generally have higher Ni contents than surface grains
12	Metal in igneous rims is dispersed and has smaller mean grain sizes than metal on surfaces
13	Metal within each igneous rim is uniform in composition
14	Some very large metal grains show Ni gradients with Ni decreasing towards the exterior
15	Moderately large surficial metal grains show marginal or no Ni gradients
16	Within chondrules, Co contents are positively correlated with Ni contents

dence of thermal metamorphism having affected CR chondrites, and because none of these features appears to be the result of asteroidal aqueous alteration or terrestrial weathering, we limit our discussion to nebular processes, particularly those associated with condensation and chondrule formation.

4.1. The geometric arrangement of metal on CR chondrule surfaces

This section deals with the first three features listed in Table 3. About half the metal in CR chondrites is in the form of large ($\geqslant$40 μm) grains located on the surfaces of chondrules, far more than in any other chondrite group. Most of the remaining metal in CR chondrites is dispersed in the interiors of chondrules or within igneous rims. A non-trivial portion is present in still-larger (200–1300 μm) grains residing in the matrix.

In Section 3.1 we noted that (in section) the typical distribution of surface metal consists of a discontinuous ring of coarse globules. As discussed above, sectioning chondrules at random angles will only yield this distribution if the surface metal is isotropically distributed. As noted earlier, such an isotropic distribution cannot be the result of centrifugal forces moving the more dense metal to the equator, because random sectioning of an equatorial distribution would rarely yield a ring-like distribution.

Our studies show that, on each chondrule, the surface metal is highly uniform in composition (as noted in Section 3.6, smaller grains have slightly lower Ni), but that the mean compositions vary from chondrule to chondrule and, for concentric compound chondrules, between different metallic "shells" in the same chondrule. Comparison of different chondrules and shells reveals that Co and Ni are positively correlated and that the Ni contents of metal are negatively correlated with the fayalite contents of the olivine. With rare exceptions, surficial metal is free of FeS and there is also no FeS in the chondrule interiors.

There seems to be only one explanation of the uniform distribution of metal on chondrule surfaces, one advanced almost five decades ago by Wood (1963): during chondrule formation the interplay of surface tension and interfacial tension caused the metal to wet the surface of the (largely molten) silicates, and the more stable arrangement was for metal to be on the outside of the assemblage. The possibility that surface tension could cause the ejection of metal droplets was recently discussed by Uesugi et al. (2008), but there is no evidence for such ejection in the CR chondrule assemblages that we are discussing. We suggest that some of the metal originally formed on the surface and that some was wicked to the surface through channels in the silicate melt or at interfaces between silicate crystals. Centrifugal forces may have augmented this process, but the final distribution was controlled by surface tension.

The behavior of the metallic and silicate systems is described by Young's equation:

$$\gamma_{sv} = \gamma_{sm} + \gamma_{mv} \cdot \cos\theta \quad (1a)$$

$$\gamma_{sv} - \gamma_{sm} = \gamma_{mv} \cdot \cos\theta \quad (1b)$$

The equation is written for the case where the volume of the silicate liquid is larger than that of the metallic melt and can thus be thought of as the substrate. We will designate the silicate the host liquid and the minor metal liquid the guest liquid. The subscript letters are s (silicate liquid), m (metal liquid) and v (vapor). The angle θ is called the contact angle. A low contact angle (e.g., <60°) corresponds to a guest liquid that efficiently wets a surface whereas a high contact angle (e.g., >120°) indicates that the guest liquid does not wet the host. A high contact angle makes the external liquid ball up; a very low angle causes the external liquid to spread across the entire substrate. The actual contact angle reflects the combination of the three surface tensions, but the sign of cos θ is determined by the left side of Eq. (1b).

We agree with the conclusion of Wood (1963) that there seems to be only one plausible way to account for the isotropic distribution of metal on the surface of CR chondrules: during chondrule formation the metallic melt wet the surface of the underlying chondrule. At that time its surface tension (γ_{mv}) was lower than that of the silicate melt (γ_{sv}), favoring its transport to the surface of the largely molten chondrule.

The cartoon sketch in Fig. 9a represents a section through the chondrule when the surface was covered by a metal film. Had the chondrule immediately been frozen at this time, the sections through CR chondrules would look like this metal configuration rather than the rings of beads that are commonly observed. We therefore infer that, while the metal was still molten, the interfacial tension between metal and silicate increased and the left side of Eq. (1b) became positive. The surface energy was then minimized by reducing the contact area between the metal and the silicate melts; as a consequence, the metal balled up. A section through the chondrule then looked like the sketch in Fig. 9b, i.e., a string of beads. The cartoons do not show the effects of off-center sectioning but these are generally relatively minor.

It is probable that the interfacial tension increased as the temperature fell, and this may be the entire reason for the metal forming the observed globules. There is, however, a second possibility. Wood (1963) suggested that FeS dissolved in the melt would decrease interfacial tension; perhaps some FeS was in the initial melt that moved from the interior of the chondrule to the surface. A recent study by Li et al. (2005) confirms that, for S contents in the range 8–500 μg/g, an increase in S decreased the sur-

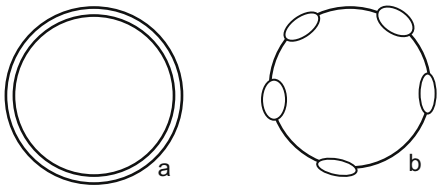

Fig. 9. (a) Sketch of a section through a chondrule covered by a film of metal; (b) sketch of metal globules that could have formed from the metal film after the interfacial tension increased during cooling.

face tension of a melt consisting of 10–20% Cr and the remainder Fe. If FeS was initially present, the gradual evaporation of the S would have produced an increase in the interfacial tension, and thus a tendency for the metal to ball up.

4.2. Origin of the low S contents of chondrules and their metallic shells

Before discussing the origin of the low FeS content of the chondrules and their surface assemblages, we note that the liquidus temperature of S-free, low-Ni metal is very high. The Fe–Ni phase diagram in Brandes and Brook (1998) shows a liquidus temperature of ~1785 K for S-free metal containing about 5% Ni.

There are two major ways to establish phase compositions and phase abundances in the solar nebula. The first is generally called condensation but, in nebular regions that are undergoing temperature fluctuations (for example, during chondrule formation) the process is actually some mix of evaporation and condensation. These processes can be roughly modeled by equilibrium processes; a handy way to assess relative volatilities is to compare 50%-condensation temperatures (Wasson, 1985; Lodders and Fegley, 1998) in a canonical (solar-composition) nebula. For most elements the condensation temperature depends on the assumed nebular pressure, but for some, including S, the 50%-condensation temperature (~660 K) is independent of pressure. At equilibrium about 1% of the nebular S is condensed at 700 K.

The absence of S (which, if present, would occur as FeS) in CR chondrules with metallic "shells" and in essentially all low-FeO (olivine Fa contents <4 mol%) chondrules thus can be explained either by the chondrules forming when the ambient nebular temperatures were >700 K or by a loss of S from the chondrules while they were at high temperatures (perhaps as high as 1750 K in the case of metal-clad CR chondrules).

Our calculations for a canonical solar nebula give equilibrium olivine Fa contents of 1.6% at 700 K, 2.6% at 650 K and 4.1% at 600 K, similar to those observed in the chondrules hosting metallic shells (Table 1). Thus, the silicate compositions are not inconsistent with the absence of FeS being the result of high ambient nebular temperatures at the time low-FeO chondrules were forming. However, because of incomplete exchange between solids and gas during brief chondrule-forming events, we cannot rule out the possibility that ambient temperatures were appreciably lower than 660 K when chondrule melting events occurred, i.e., that silicate compositions largely preserve those of the precursor solids.

At high temperatures, FeS does not evaporate as a molecule; instead it dissociates and S enters the vapor. Dissociation of FeS thus added Fe to the metal of the system. This is one possible source of the extra Fe needed to produce the positive correlations between Co and Ni in CR metal. Zanda et al. (2002) suggested that this process occurred during the formation of ordinary-chondrite chondrules.

4.3. Origin of the compositional trends in the surficial coarse metal of CR chondrites

The uniform composition of surface metal (Table 1; 95% uncertainties in Fig. 4) on each chondrule seems to be precisely what one would expect if (most of) the surface metal migrated from the interior to the surface through channels, and remained molten on the surface for an appreciable length of time. The molten metal would have mixed both during the mechanical flow to form the surficial film and by diffusion at the high temperatures present during chondrule formation. At a temperature of 1750 K the diffusion coefficient of Ni in a metallic melt is probably between 10^{-7} and 10^{-8} m^2 s^{-1}; thus, in a time of ~10 s the Ni can diffuse a distance of about 40–100 μm. As a result, the original compositional scatter in the chondrule precursor grains should have been reduced by a factor of several during the formation of the metallic film (and then the molten globules).

The platinum-group-element data of Connolly et al. (2001) are inconsistent with the situation described in the previous paragraph; they reported large PGE variations among the ring grains of a single chondrule. For example, in "chondrule 8 large sibling from PCA 91082" they report an Ir range of a factor of 8, an Os range of a factor of 13 and a Au range of a factor of 1.8, even though the relative errors are estimated to be only ±10%. The technique Connolly et al. (2001) employed, the ion-microprobe, is not well suited to the analysis of PGE elements because ion yields are highly variable. In the previous paper by Hsu et al. (2000), ranges of factors of two are reported for PGE elements in iron meteorite standards including two hexahedrites.

Humayun et al. (2010) used laser-ablation ICP-MS to study some of the metal grains analyzed by Connolly et al. (2001); they also found moderately large ranges in elemental abundances and especially those of refractory siderophiles. For most grains the ranges are by factors <2, but siderophile concentrations in some exceptional grains are two to five times above or below the mean composition. Thus, a complete model for the formation of the metal-cladding on the CR chondrules must include a mechanism to account for grains having anomalous compositions.

Humayun et al. (2010) suggested that high and low contents of siderophiles were produced by fractional crystallization. Another possibility is that the anomalous points are loci where unmelted nebular grains became embedded in the surficial film of melt.

As discussed in connection with Fig. 7, at a level of ±0.1 wt.% we did not observe any Ni gradients within three moderate-size (55–100 μm) individual grains that were parts of rings. The gradient that was observed in a metal globule with a thickness of 600 μm is discussed below; we attribute this gradient to fractional crystallization. More data are needed to assess the relative merits of the two scenarios, fractional crystallization versus contamination by nebular grains.

The compositional variations among chondrules shown in Fig. 4 were not unexpected because each chondrule records stochastic variations in the compositions of precursor materials that might include metal grains that formed (by evapo-

ration and condensation) over a range of temperatures as well as metal from earlier generations of chondrules.

Past papers (e.g., Weisberg et al., 1993; Connolly et al., 2001) have noted that there is a strong correlation between Co and Ni in CR metal. As shown in Fig. 5a, we also confirm this covariation in our ring metal samples. A reference line shows an (arbitrary) constant Co/Ni ratio. The trend through the data clearly shows a lower slope, but there is too much scatter to rule out a constant ratio. The scatter partly results from sampling errors but analytical errors are also large because Co concentrations are low and corrections for the Fe K_β interference are typically about as large as the reported values. Note that, in the two cases where we studied two rings in the same chondrule, the inner ring has the higher Co and Ni contents. Although we do not include coarse interior metal compositions in Fig. 5a, with rare exceptions, coarse interior metal has higher Ni contents than the ring metal on the surface of the chondrules.

Because Co and Ni show opposite partitioning between kamacite and taenite, the covariation cannot be explained by stochastic sampling of these phases. The common hypothesis is that it is a condensation effect (with the first metal having high contents of Co and Ni and the last condensate metal having low contents of these elements). Other hypotheses involve reduction of FeO from surrounding silicates during mild metamorphism (Lee et al., 1992) or loss of S from FeS during chondrule formation (e.g., Zanda et al., 1995; Hewins et al., 1997).

Our present view is that FeO reduction during metamorphism cannot be the explanation for the Co–Ni covariation. Although Lee et al. (1992) suggested that FeO reduction occurred on the parent asteroid, we now rule this out because there is little or no evidence of thermal metamorphism in CR chondrites. Reduction could have occurred in the nebula during chondrule melting, perhaps abetted by a reducing agent such as graphite (Connolly et al., 2001), but this would affect only the melted materials (which we later estimate to be 50% to 75% of the total silicates). During this brief event no Fe would be transferred out of the unmelted silicates. As discussed above, almost all of the chondrules are porphyritic, implying that some may have grown around coarse precursors. That we have never observed FeO-rich cores in BSE images of metal-clad chondrules weighs against this model.

As noted in Section 3.2, we observe a negative correlation between the Ni in the metallic rings and olivine Fa contents in the host silicates. This is the opposite trend to that expected if the range in Ni is the result of reducing FeO from the precursor silicates during chondrule formation. Another fact that argues against *in situ* reduction is our observations of LAP chondrule F3o. Here, the two coarse metal rings show large differences in mean Ni content; the primary (inner) ring contains 7.2% Ni, the outer ring 5.4%. If these were produced by large degrees of FeO reduction, we would expect the silicates inside the outer ring to be much more reduced than those inside the (primary) inner ring. In fact, their mean olivine compositions are only marginally different (Fa1.3 in the primary chondrule, Fa1.4 in the enveloping secondary). We thus conclude that reduction of coexisting silicates during chondrule formation was not the main process responsible for the Co–Ni correlation in the metal.

Connolly et al. (2001) suggested that some refractory-poor, Fe-rich metal on chondrule surfaces formed by recondensation of Fe evaporated during chondrule formation. Because during rapidly falling temperatures condensation occurs on any available surface and most of the surface is on fine grains, we are confident that this scenario cannot be correct. There is no evidence implying that an appreciable fraction of the metallic Fe evaporated and no reason to believe that an appreciable fraction of evaporated material recondensed on chondrule surfaces.

There appear to be only two ways in the solar nebula to separate Fe from the main host phase(s) of Ni and Co: (a) separation during nebular condensation, and (b) separation during volatilization associated with chondrule formation at low ambient nebular temperatures.

As pointed out by numerous authors (e.g., Weisberg et al., 1993), Ni and Co are slightly more refractory than Fe, and are expected to be concentrated in the first condensate of high-temperature nebular metal. If this high-temperature metal is isolated from later condensed metal that has low-Ni and Co contents, positive correlations would result from mixing of these two metallic nebular components.

The second alternative is more complicated, but at least equally plausible. During chondrule formation, chondrule temperatures are typically about 600 K higher than the vaporization temperature of metallic Fe (and ~1200 K above the volatilization temperature of FeS). As discussed by various authors (e.g., Wasson, 2008) the volatilized material immediately recondenses as homogeneously formed smoke particles or on the surfaces of preexisting fine grains. Because the overwhelming fraction of the available surface is on grains with sizes <10 μm, very little of this vaporized material recondenses on the surfaces of chondrules. Mild reheating of the smoke particles would be expected to result in bonding between the Fe and either O or S. The next generation of chondrule precursor materials would thus be expected to have a larger fraction of the Fe in the form of FeS and FeO than was present in the previous chondrule generation. If large metal grains were not fully melted in the new chondrule, the unmelted metal should have higher Ni and Co than the molten fraction. All the FeS should be in the molten fraction.

If the first (fractional condensation) model is correct, then the same process needs to occur during chondrule melting; the melt needs to be enriched in the late condensate. This late-condensing Fe would have had a finer grain size and have contained a larger fraction of FeS relative to the earlier metal condensate. Thus, as in the other nebular model, the metallic melt would be expected to have a lower Ni content than residual metallic solids.

We note that, given the low S content of CR chondrule metal, equilibrium partial melting would produce the opposite effect to that observed. In metallic melts having low S contents, the solid has a lower Ni content than the coexisting melt. The solid/melt ratio is expected to be in the range 0.8–0.9 (e.g., Chabot and Jones, 2003). Thus, any metal

remaining as a solid residue after partial melting should have lower Ni than the melt.

4.4. Coarse metal in chondrule interiors and in igneous rims

As noted by earlier authors, the coarse metal in chondrule interiors commonly has higher Ni contents than the metal shells on the surface. In this study we gathered data on 11 primary metal rings (or shells); in six of these, coarse metal grains were present in the host chondrule. In each of these cases the coarse metal was more Ni rich than that in the surrounding shell. The nearest thing to an exception was the second set of grains in F3o with a mean composition only 0.2% higher in Ni than that in the surrounding shell. We also studied metal grains between the rings of F3o and found it to have higher Ni contents intermediate between those in the inner and outer rings.

We suggest that the high-Ni grains remained largely unmelted during the melting event that formed the overlying metallic shell. They may have been coarse relicts from a previous episode of chondrule formation. This presents a challenge in the sense that the liquidus temperature decreases with increasing Ni content of FeNi metal (up to about 45% Ni). If, as suggested in the model in Section 4.1, most of the shell metal came to the surface during the melting event that formed both the host chondrule and the metallic shell, we must explain why that metal melted but the high-Ni relicts remained solid. We propose two possibilities: (a) temperatures were moderately low, and the metal that reached the surface was fluxed by FeS, or (b) large metal grains were heated only by conduction (and not by compression) and that the heat transport was too slow to melt all large metal grains. Because heat conduction in metals is rapid, we consider fluxing by FeS the more probable explanation. Although FeS–Fe melts can form at temperatures as low as 1260 K, the temperature must have been much higher when the metal moved to the surface of the chondrule because (a) the viscosity must have been quite low, and (b) a moderate amount of the silicates must have been molten.

As discussed in Section 4.1, the presence of FeS also enhances the ability of the melt to wet the silicates. And, if the heat pulse was long enough to dissociate the FeS and evaporate the S, this would increase the Fe content of the surficial metal and would eventually cause the melt-silicate contact angle to rise and the metal to form globules.

Because of their convoluted outlines, we infer that the igneous rims contained more unmelted silicate phenocrysts than the chondrules having smooth exteriors. This implies a shorter heat pulse and thus also less time for the metal to migrate to the surface. Although some metal compositions in igneous rims are as uniform as those in the rings, others are quite heterogeneous. The relative standard deviation for Ni in the igneous rim of A59 I4b is ~12%, considerably larger than the largest in a ring (~8%). Nonetheless, the relatively low degree of scatter observed in the coarse metal in these rims is then evidence that compositional variations in the precursor mix was also relatively small.

Some of the chondrules with convoluted margins have small arcs of exterior metal that may be nascent metallic shells. Following this line of thought, we conclude that the remaining metal in these convoluted chondrules has essentially not moved during the chondrule melting event. The mean viscosity was too high. The squiggly shape show that the metal was soft enough to be easily deformed, but appreciable flow did not occur.

4.5. Origin of the compositional trends within large metal grains

In Section 3.4 we described a profile (Fig. 8) across a 600-μm-wide metal grain in A97 chondrule N4n (Fig. 2d). We suggested that the lower Ni content at the external surface was produced by fractional crystallization. We rejected the alternative, that evaporation of Fe during chondrule formation resulted in the recondensation of low-Ni metallic Fe (Connolly et al., 2001), in part because such recondensation should occur on all grain surfaces, and thus preferentially on small dust grains rather than on millimeter-size chondrules. In addition, we would expect the dilution by such a process to be most effective for small metallic masses on the chondrule surface; however, as also reported by Lee et al. (1992), this effect has only been observed in very large grains.

The proposed fractional-crystallization process starts when the metal cools and nucleates following the brief heat impulse that melted the chondrule. The exterior surface of the drop would have been the first part to fall to the liquidus temperature; solid metal would have nucleated. Because of its large size, cooling of grain N4n would have been slower than the smaller metal grains on chondrule surfaces, thus increasing the time available to mix the residual melt.

To assess whether the trend is consistent with fractional crystallization we need to know the mean Ni content of the metal grain. We will assume that the shape is hemispherical and that the surface in contact with the silicates corresponds to an equatorial slice through the corresponding sphere. This indicates that more than half the metal is in the outer 25% of the radius; we therefore roughly estimate the mean Ni content of the metallic grain to be 5.4 wt.%.

There is relatively little uncertainty regarding the solid/liquid distribution coefficient (D value) in a metallic melt having a low S content; the value is surely in the range 0.8–0.9. The Ni–Au data for the low S group-IVA iron meteorites (Wasson et al., 2006) correspond well to a D_{Ni} value of 0.89. This D value leads to the expectation that the first metal to crystallize would have a Ni content of ~4.8 wt.%, similar to the outermost values in the profile shown in Fig. 8. (Surficial Ni could have been slightly lower, but we were unable to study the actual surface because it had been replaced by a corrosion layer.)

In principle, the Co profile offers a test of the fractional crystallization model. Unfortunately, our data (Fig. 8) scatter too much to be useful for this purpose. The trend for Co should be similar to that for Ni but with a lower gradient; our fit to the Co–Au trend in IVA irons yields a rough D_{Co} value of 0.95.

We conclude that fractional crystallization offers the best explanation for the trend. This requires that the

remaining melt remained reasonably well mixed as crystallization continued.

In order to produce appreciable (if non-ideal) fractional crystallization one needs to mix the residual liquid several times during crystallization of the grain. In Section 4.3 we showed that Ni can diffuse 40–100 μm in 10 s at the liquidus temperature of about 1750 K. Any convecting motions that occurred would have reduced the time required for mixing. Thus, if the cooling rate were slow enough that it took >40 s for 80% of the metal to crystallize, an appreciable degree of fractional crystallization should have occurred.

5. DISCUSSION SUMMARY: ORIGIN OF THE MAIN METAL COMPOSITIONAL TRENDS; IMPLICATIONS FOR CHONDRULE FORMATION IN THE CR REGION

The coarse metal in CR chondrites appears to have been affected by three independent processes: (a) fractional crystallization of the largest metal masses, with the earliest crystallizing metal achieving the lowest Ni contents; (b) formation of metal with high-Ni and Co in the solar nebula, probably because of processes related to the higher volatility of Fe; and (c) dilution of high-Ni metal by low-Ni metal during chondrule formation; smaller grains experienced more dilution than larger grains, implying the deposition of low-Ni metal on grain surfaces followed by incomplete homogenization.

5.1. Fractional crystallization of large metal grains on chondrule surfaces

The fractional-crystallization process is probably the least interesting and the least controversial. The large Ni gradient near the outside of the largest grains seems to be straightforwardly explained by (non-ideal) fractional crystallization. Nucleation occurred first on the outside surface, and the remaining melt mixed by diffusion and possibly also by convection. We assumed that the grain had a hemispherical shape and that crystallization occurred on the entire outer, 2π steradian geometry; this accounts for the much higher gradient near the surface.

Smaller (ca. 100 μm) metal grains do not show resolvable gradients. In part because these grains are relatively thin (50–100 μm in a chondrule radial direction), they crystallized too rapidly to permit mixing of the residual melt.

5.2. Ni–Co correlations and the fractionation of siderophiles in the solar nebula

There are two reasons to believe that the CR chondrules preserve at least a partial record of nebular evaporation/condensation. The first is the gradual increase in Ni from center to edge of compound chondrules such as LAP F3o; the second is the negative correlation between Ni in the ring metal and the fayalite (FeO) content of the olivine in the host chondrule for the full set of metal-clad chondrules. This is the opposite of the "Prior's rule" type of fractionation in which redox differences affect the distribution of Fe between oxidized and reduced states. In the latter case, redox processes resulting in a larger fraction of reduced Fe were responsible for lowering both the Ni content of the metal and the olivine Fa content.

The negative trend between ring metal Ni and chondrule olivine Fa is consistent with the following qualitative nebular mixing model in which chondrules appear to consist of a mix of early, higher-temperature materials and late, lower-temperature materials. Because Ni and Co are more refractory than Fe, high-temperature materials (condensates or evaporation residues) are expected to have relatively high-Ni and Co contents. High-temperature silicates have low-FeO contents. The high-temperature component thus would be a mix of high-Ni metal and low-FeO silicates.

The second constraint on the Ni, Co and olivine Fa correlations is that there is commonly a time sequence recorded in compound chondrules. The inner (primary) chondrule contains a larger proportion of the high-temperature component than the secondary chondrule, consistent with a scenario in which there is a gradual drift in the composition of nebular solids corresponding to a decrease in ambient nebular temperatures. The precursors of the earlier-formed chondrules contained a higher fraction of high-temperature nebular solids than the later-formed chondrules.

As the nebula cooled and some materials were recycled (probably by melting and evaporation in chondrule-forming events) the Ni/Fe ratio in the metal would have gradually moved closer to the solar ratio and the FeO content of the silicates would have gradually increased (though, in the case of the actual components that went into the CR metal-clad chondrules, the required increase in the latter was minor, from about olivine Fa1 to about Fa3). It should be noted that for reasons of kinetics and stochastic brief heating events (chondrule-forming events) there would have been a range of olivine Fa contents at each ambient nebular temperature, with the mean value gradually increasing as the ambient temperature decreased.

5.3. The high-temperature pulse recorded in low-FeO CR chondrules

The remarkably low FeS content of CR chondrules was mentioned by Weisberg et al. (1993) and documented with S maps by Wasson and Rubin (2009) and Wasson (2008). As noted above, the evidence that metal flowed on the surface of CR chondrules and the observed absence of FeS in the metal allow us to calculate that the metal reached temperatures of ~1750 K. Although this is below the liquidus temperature, nucleation barriers hinder the crystallization of metallic liquids; thus, the liquids could have persisted long enough to ball up. If there were any grains of unmelted nebular metal on the surface, these could have facilitated the eventual crystallization.

The heat pulse was surely long enough to cause all the FeS in the melt to be lost. The same appears to be true for any FeS that was initially incorporated into the chondrule. When the surficial film of metal lost its S, it balled up (as a result of the increase in interfacial tension).

We roughly estimated the temperature necessary to achieve appreciable melting of the silicates. We estimated

a mean composition of low-FeO CR chondrules by starting with the bulk CR compositional data of Kallemeyn et al. (1994) and augmenting it with 153 mg/g Si, an element not determined in that study. We then assumed that, relative to this composition, the low-FeO chondrules contained only 10% of the Na, K (the remainder is in the vapor) and Fe (the remainder is not bound to O). Using the MELTS program (Ghiorso and Sack, 1995), we calculated the melt fractions (in parentheses) at temperatures of 1700 K (49%), 1750 K (53%), 1800 K (61%) and 1850 K (70%). For this composition complete melting occurred at 1948 K. Thus, at our suggested temperature of 1750 K, about 50% of the silicates were molten.

Note that the preservation of the textures of the primary chondrules demonstrates that these experienced much lower degrees of melting at the time temperatures were high enough to allow the separation of a metallic liquid in the secondary chondrule. This fits with the general concept that it is mainly the fine materials that were melted during the formation of low-FeO chondrules.

Ten of the metal-clad chondrules are porphyritic and one is barred olivine. As discussed above, the mafic minerals in some of the porphyritic chondrules are relatively coarse with little intervening mesostasis. We describe portions of them as "granoblastic". This coarse texture seems to reflect relatively long exposure to high temperatures. Thus, both the absence of FeS and the granoblastic silicates imply that these chondrules spent a relatively long period at high (ca. 1800–1700 K) temperatures.

We suggest that the chondrule-forming events that produced the low-FeO CR chondrules were qualitatively different from those that formed low-FeO chondrules in other chondrites. Assuming that the same physical mechanism was responsible for flash melting chondrules at all locations, longer pulses might be expected if the ambient temperatures were higher and if the chondrule formation regions were opaque enough that a sizable fraction of the IR photons underwent absorption rather than immediately escaping. As discussed by Wasson and Rubin (2003), large phenocrysts seem to have formed in a series of flash-heating events, most of which melted only mesostasis. If each of these heat pulses were longer, a larger fraction of porphyritic chondrules would be expected to show granoblastic textures.

Documentation of the inferred differences in chondrule properties and thus the differences in chondrule formation conditions at different nebular times or places will require much effort, but it is through such documentation that proper constraints on chondrule formation can be provided.

ACKNOWLEDGMENTS

This research was largely supported by NASA grant NNG06GG35G (JTW) with additional support by NASA grant NNG06GF95G (AER). We thank Frank Kyte for assistance with electron-microprobe studies and Tram Le for help with data reduction and image preparation. Samples were kindly provided by C. Satterwhite for the Meteorite Working Group, A. Greshake of the Humboldt Museum in Berlin, and M. Prinz of the American Museum in New York. We are grateful to A. Kracher and M. Humayun for useful and supportive reviews.

APPENDIX A. SUPPLEMENTARY DATA

Supplementary data associated with this article can be found, in the online version, at doi:10.1016/j.gca.2010.01.014.

REFERENCES

Brandes E. A. and Brook G. B. (1998) *Smithells Metal Reference Book*. Butterworth-Heinemann, ca, 1600 pp..

Chabot N. L. and Jones J. H. (2003) The parameterization of solid metal–liquid metal partitioning of siderophile elements. *Meteorit. Planet. Sci.* **38**, 1425–1436.

Connolly, Jr., H. C., Huss G. I. and Wasserburg G. J. (2001) On the formation of Fe–Ni metal in Renazzo-like carbonaceous chondrites. *Geochim. Cosmochim. Acta* **65**, 4567–4588.

Ghiorso M. S. and Sack R. O. (1995) Chemical mass transfer in magmatic processes. IV. A revised and internally consistent thermodynamic model for the interpolation and extrapolation of liquid–solid equilibria in magmatic systems at elevated temperatures and pressures. *Contrib. Mineral. Petrol.* **119**, 197–212.

Grossman J. N. and Wasson J. T. (1985) The origin and history of the metal and sulfide components of chondrules. *Geochim. Cosmochim. Acta* **49**, 925–939.

Hewins R. H., Yu Y., Zanda B. and Bourot-Denise M. (1997) Do nebular fractionations, evaporative losses, or both, influence chondrule compositions? *Antarct. Meteorite Res.* **10**, 275–298.

Hsu W., Huss G. I. and Wasserburg G. J. (2000) Ion probe measurements of Os, Ir, Pt, and Au in individual phases of iron meteorites. *Geochim. Cosmochim. Acta* **64**, 1133–1147.

Humayun M., Campbell A. J., Zanda B. and Bourot-Denise M. (2002) Formation of Renazzo chondrule metal inferred from siderophile elements (abstract). *Lunar Planet. Sci.* **33**, #1965 (abstr.).

Humayun, M., Connolly, H. C., Rubin, A. E. and Wasson, J. T. (2010) Elemental distribution in metal from the CR chondrites Acfer 059 and PCA 91082. *Lunar Planet. Sci.* **41**, #1840 (abstr.).

Kallemeyn G. W., Rubin A. E. and Wasson J. T. (1994) The compositional classification of chondrites: VI. The CR carbonaceous chondrite group. *Geochim. Cosmochim. Acta* **58**, 2873–2888.

Kong P., Ebihara M. and Palme H. (1999) Distribution of siderophile elements in CR chondrites: evidence for evaporation and recondensation during chondrule formation. *Geochim. Cosmochim. Acta* **63**, 2637–2652.

Kong P. and Palme H. (1999) Compositional and genetic relationship between chondrules, chondrule rims, metal, and matrix in the Renazzo chondrite. *Geochim. Cosmochim. Acta* **63**, 3673–3682.

Lee M. S., Rubin A. E. and Wasson J. T. (1992) Origin of metallic Fe–Ni in Renazzo and related chondrites. *Geochim. Cosmochim. Acta* **56**, 2521–2533.

Li Z., Mukai K., Zeze M. and Mills K. C. (2005) Determination of the surface tension of liquid stainless steel. *J. Mater. Sci.* **40**, 2191–2195.

Lodders K. and Fegley B. J. (1998) *The Planetary Scientist's Companion*. Oxford Univ. Press, New York, 371 pp..

Rubin A. E. and Wasson J. T. (2005) Non-spherical lobate chondrules in CO3.0 Y-81020: general implications for the formation of low-FeO porphyritic chondrules in CO chondrites. *Geochim. Cosmochim. Acta* **69**, 211–220.

Uesugi M., Sekiya M. and Nakamura T. (2008) Kinetic stability of a melted iron globule during chondrule formation. I. Non-rotating model. *Meteorit. Planet. Sci.* **43**, 717–730.

Wasson J. T. (1985) *Meteorites: Their Record of Early Solar System History*. Freeman, 267 pp.

Wasson J. T. (2008) Evaporation of nebular fines during chondrule formation. *Icarus* **195**, 895–907.

Wasson J. T., Matsunami Y. and Rubin A. E. (2006) Silica and pyroxene in IVA irons; possible formation of the IVA magma by impact melting and reduction of L-LL-chondrite materials followed by crystallization and cooling. *Geochim. Cosmochim. Acta* **70**, 3149–3172.

Wasson J. T. and Rubin A. E. (2003) Ubiquitous low-FeO relict grains in type-II chondrules and limited overgrowths on relicts and high-FeO phenocrysts following the final melting event. *Geochim. Cosmochim. Acta* **67**, 2239–2250.

Wasson J. T. and Rubin A. E. (2009) Composition of matrix in the CR chondrite LAP 02342. *Geochim. Cosmochim. Acta* **73**, 1436–1460.

Weisberg M. K., Prinz M., Clayton R. N. and Mayeda T. K. (1993) The CR (Renazzo-type) carbonaceous chondrite group and its implications. *Geochim. Cosmochim. Acta* **57**, 1567–1586.

Wood J. A. (1963) On the origin of chondrules and chondrites. *Icarus* **2**, 152–180.

Zanda B., Bourot-Denise M. and Hewins R. H. (1995) Condensate sulfide and its metamorphic transformations in primitive chondrites (abstract). *Meteoritics* **30**, 605.

Zanda B., Bourot-Denise M., Hewins R. H., Cohen B. A., Delaney J. S., Humayun M. and Campbell A. J. (2002) Accretion textures, iron evaporation and re-condensation in Renazzo chondrules (abstract). *Lunar Planet. Sci.* **33**, #1852 (abstr.).

Associate editor: Christian Koeberl